CREB1 contributes colorectal cancer cell plasticity by regulating lncRNA CCAT1 and NF-κB pathways

Authors:

Bin Li[1], Li-Si Zheng[2], Chen-Min Zhang[1], Qiao-Juan Huang[1], Yan-Hua Guo[3], Lu-Qin Wang[4], Peng Yu[1], Shu-Rong Liu[1], Qiao Lin[1], Yu-Xia Luo[1], Hui Zhou[1], Jian-Hua Yang[1,5,†] and Liang-Hu Qu[1,†]

Affiliation:

[1] MOE Key Laboratory of Gene Function and Regulation, State Key Laboratory for Biocontrol, School of Life Sciences, Sun Yat-sen University, Guangzhou, 510275, China;

[2] Sun Yat-sen University Cancer Center, Guangzhou 510060, China;

[3] Guangzhou Quality Supervision and Testing Institute, Guangzhou 511400, China;

[4] Guangzhou Institutes of Biomedicine and Health, Chinese Academy of Sciences, Guangzhou 510663, China;

[5] The Fifth Affiliated Hospital, Sun Yat-sen University, Zhuhai, 519000, China

[†] **Correspondence to:**

Liang-Hu Qu, **e-mail**: lssqlh@mail.sysu.edu.cn

Jian-Hua Yang, **e-mail**: yangjh7@mail.sysu.edu.cn

Abstract

The CREB1 gene encodes a pleiotropic transcription factor that frequently dysregulated in cancers. CREB1 can regulates tumour cell status of proliferation or migration, however, the molecular basis for this switch involvement in cell plasticity has not been fully understood. Here, we show that knocking out CREB1 triggered a remarkable effect of epithelial-mesenchymal transition (EMT) and led to the occurrence of inhibited proliferation and enhanced motility in cancer cells. Mechanistically, CREB1-knockout cells showed arrest in the G0/G1 phase as a result of impaired CREB1-dependent transcription of CCAT1 and E2F1. Interestingly, the competition between the coactivator CBP/p300 for CREB1 and p65 leads to the activation of the NF-κB pathway in cells with CREB1 disrupted, which induces an EMT phenotype and

enhances motility. These studies identified previously unknown mechanisms of CREB1 in cell plasticity via its lncRNA and protein effector pathways, revealing an important feature that should be considered in CREB1-targeted tumour therapies.

Key words: CREB1, cell plasticity, CCAT1, NF-κB pathway, Cell cycle, EMT

Introduction

Cancer cells are associated with a high degree of cellular plasticity that includes molecular and phenotypic changes during tumour progression and treatment (Yuan et al., 2019). Increasing evidence suggests that cancer cells undergo phenotypic switching between growth and metastasis phenotypes in response to genomic or epigenetic alteration as well as a volatile microenvironment. Indeed, studies indicate that oncogenic genes with paradoxical functions can contribute the capacity for phenotypic plasticity. For example, *c-myc*, a well-known oncogene, can stimulate the proliferation of breast cancer cells both in culture and *in vivo*, but it can inhibit motility and invasiveness in culture and lung or liver metastases in xenografted tumours (Hong et al., 2012). Thus, the opposite role of oncogenes that can promote proliferation pathways but simultaneously suppress migration pathways might be an intrinsic mechanism of cancer cell plasticity in tumours. However, how genes with paradoxical functional role involve in cellular plasticity need to be addressed.

The oncogene *CREB1* encodes an exceptionally pleiotropic transcription factor (CREB1) that bind to promoter *cis*-regulatory elements (CREs) which are composed of TGANNTCA sequences, is ubiquitously expressed in many tissues (Impey et al., 2004, Zhang et al., 2005). Furthermore, CREB1 has been reported to regulate both coding and noncoding genes that are generally involved in the regulation of cell survival, proliferation and glucose metabolism (Lonze and Ginty, 2002, Carlezon et al., 2005, Wang et al., 2010, James et al., 2009, Fusco et al., 2016).

Elevated expression of CREB1 in multiple tumours including acute myeloid leukaemia, prostate cancer, gastric cancer and gliomas, is associated with enhanced cell proliferation (Shankar et al., 2005, Zhang et al., 2011, Rao et al., 2017, Tan et al., 2012). Paradoxically, such overexpression is dissociated from invasive and metastatic propensity, and the inhibition of CREB1 accounts for the increase of cell invasiveness (Guo et al., 2016a, Bian et al., 2016).

These studies demonstrated contradictory effects of CREB1 on tumour progression, which raise the possibility that CREB1 could contribute tumour cell plasticity by switching from a proliferative to an invasive state. However, the molecular mechanisms which mediated the switch between proliferation and invasion of cancer cells are poorly understood.

Here, we investigated the impact of CREB1 on cell phenotypic plasticity and demonstrated paradoxical effects of CREB1 on cell proliferation and motility, using CRISPR/Cas9-mediated CREB1-knockout HCT116 cells. In particular, we elucidated the molecular mechanisms of CREB1 on cell plasticity by regulating lncRNA CCAT1 and NF-κB pathways. Our findings have uncovered a previously unappreciated function of CREB1 for the control of tumour cells between proliferation and metastatic states with its coding and noncoding effector pathways, which reveals a mechanism that may be important in the development of therapeutics that target CREB1.

Results

CREB1 deletion impairs cell proliferation and increases migration and invasion

In an effort to examine the effects of CREB1 ablation in HCT116 cells, we used CRISPR/Cas9n technology with a pair of offset sgRNAs (sgRNA-C1 and C2) complementary to opposite strands of exon 5 to knock out CREB1 (Supplementary figure 1A) (Ran et al., 2013). sgRNA-C1 and C2 were cloned into PX462, a bicistronic vector that contains the Cas9n enzyme and a programmable chimeric sgRNA. To increase the efficiency of indel mutations, the sgRNA-C2 transcript unit (U6-promoter-sgRNA-C2) was subcloned into the PX462-sgRNA-C1, resulting in the tricistronic vector PX462-C1C2 (Supplementary figure 1B). The effectiveness of PX462-C1C2 was evaluated by T7E1 nuclease assay, and the efficiency of introducing indel mutations at the exon 5 target site reached up to 90% (Supplementary figure 1C). Then, we performed a serial dilution to isolate single CREB1 knockout clones. Twenty-two clones were probed for the T7E1 nuclease assay, and eight clones were selected for additional Western blot and Sanger sequencing analyses. Compared to the unedited HCT116 cells, there was a clone (referred to as KO-CREB1) that showed a complete absence of CREB1 expression (Supplementary figure 1D and 1E).

92 To further evaluate whether the isolated clone was functionally CREB1 deficient, CREB1
93 signaling pathway activity and CREB1-associated genes (including CREB family genes and
94 coactivators) were measured. As expected, the CREB1 signaling pathway was repressed in
95 response to CREB1 depletion, as indicated by the significant decreased in CREB1 reporter
96 activities and in the expression of the CREB1 target genes NR4A1, CYP19A1, BRCA1, BCL2
97 and cFos (Figure 1A and 1B) (Lemberger et al., 2008, Michael et al., 1997, Ghosh et al., 2008,
98 Wilson et al., 1996, Berkowitz et al., 1989, Lee et al., 1995). Disruption of CREB1 did not affect
99 the transcription of ATF1, CRTC1, CBP and EP300, whereas there was an approximately 4-
100 fold increase in CREM and a marginal decrease in CREB1 (Figure 1C) (Hummler et al., 1994).
101 Collectively, these data confirm the generation of KO-CREB1 cells using the CRISPR/Cas9n
102 system.
103 Using CCK-8 and colony formation assays, we found that knockout of CREB1 significantly
104 inhibited HCT116 cell proliferation (Figure 1D and 1E). Flow cytometry was used to assess
105 whether the absence of CREB1 in HCT116 cells was associated with changes in the proportion
106 of cells in each phase of the cell cycle. As shown in Figure 1F and 1G, the percentage of KO-
107 CREB1 cells in G0/G1-phase was significantly increased compared with that of the wild-type
108 HC116 cells during nocodazole treatment and untreated. In addition, we exogenously
109 introduced CREB1 to confirm its function in cell proliferation and the cell cycle (Supplementary
110 figure 1F). Consistent with the knockout experiments, rescue of CREB1 in KO-CREB1 cells
111 resulted in enhanced cell proliferation and G1/S transition (Supplementary figure 1G). However,
112 ectopic expression of CREB1 in wild-type HCT116 cells had no influence on cell proliferation or
113 cell cycle progression (Figure 1H and Supplementary figure 1G). In addition, disruption of
114 CREB1 in HCT116 cells did not lead to cell apoptosis or cell death (Supplementary figure 1H).
115 Upon detecting the phenotypic change of the KO-CREB1 cells, we found that the absence
116 of CREB1 induced an obvious morphological change in the cells, from an epithelial-like shape
117 to a spindle shape, meaning that CREB1 might contribute to cell motility (Figure 1I). We next
118 studied whether CREB1 ablation was involved in promoting the metastatic phenotype in
119 HCT116 cells. *In vitro* transwell assays showed a 2-fold increase in the migration and invasion
120 of KO-CREB1 cells (Guo et al., 2016a) . More importantly, overexpression of CREB1 in both
121 wild-type and KO-CREB1 cells produced only a small number of migrating and invading cells

122 (Figure 1J and 1K).

123 Taken together, these data demonstrate that disruption of CREB1 in HCT116 cells by the
124 CRISPR/Cas9n system impairs cell proliferation by accumulating cells in the G0/G1 phase, but
125 it increases migration and invasion, leading to remarkable EMT *in vitro*.

126

127 **Knockout of CREB1 alters multiple signaling pathways related to cell status**

128 To further identify the gene pathways and molecular signatures that were altered upon
129 knockout of CREB1, we conducted strand-specific RNA sequencing (ssRNA-seq) comparisons
130 of wild-type and KO-CREB1 cells. Briefly, we identified 328 genes with significant differential
131 expression (RSEM-EB-seq, 0.95 PPDE) between the wild-type and KO-CREB1 cells (Figure
132 2A, Supplementary table 1). In addition, GSEA confirmed that genes in the cAMP pathway were
133 enriched in wild-type cells (Figure 2B).

134 To obtain a global overview of the biological functions of dysregulated genes upon
135 knocking out CREB1, we performed functional annotation using Metascape analysis for Gene
136 Ontology and Protein-protein Interaction (Tripathi et al., 2015). In addition to the GO terms and
137 pathways previously associated with CREB1, such as “cell proliferation”, “positive regulation of
138 transcription from RNA polymerase II promoter” and “TGF-beta signaling pathway”, we
139 observed enrichment of genes involved in “extracellular matrix”, “cell adhesion”, “regulation of
140 actin cytoskeleton” and “ECM-receptor interaction” (Figure 2C, 2D and 2E). Interestingly, these
141 extracellular matrix-associated GO terms and pathways were in line with the role of CREB1
142 observed in the invasive KO-CREB1 cells.

143 Another method, 45-Pathway Reporter Arrays, was used to simultaneously assess 45
144 different signaling pathways in CREB1 knockout HCT116 cells. As expected, the CREB1
145 pathway exhibited the most prominent decrease when comparing knockout with wild-type
146 HCT116 cells. More interesting, many other pathways involved in cell growth, such as hypoxia,
147 MEF2, TGF-beta, and MYC, declined significantly in knockout cells. In contrast, INF, LXR, and
148 NF-κB were largely upregulated, showing intrinsic immune and inflammatory activation (Figure
149 2F).

150

151 **CREB1 facilitates the G1/S transition by transactivation of CCAT1 and E2F1**

152 To characterize the mechanism by which knockout of CREB1 induced G0/G1 arrest, we
153 analysed the expression of 15 genes involved in the G1 phase and G1/S transition in wild-type
154 HCT116 and KO-CREB1 cells. As shown in Figure 3A and 3B, E2F1, a gene known to be
155 important in cell cycle progression, was decreased in KO-CREB1 cells, and the expression of
156 cell cycle inhibitors, CDKN2B (p15), CDKN2A (p21) and CDKN1A (p27), was markedly induced
157 in KO-CREB1 cells. Intriguingly, CCND1 (Cyclin D1) and CCNE1 (Cyclin E1), which have been
158 reported to be transcriptionally regulated by CREB1 (Lee et al., 1999, D'Amico et al., 2000,
159 Nagata et al., 2001, Boulon et al., 2002), did not change in either RNA or protein levels in KO-
160 CREB1 cells.

161 Because of CREB1's central role in transcription, we compared genes whose expression
162 was downregulated in KO-CREB1 cells with CREB1-occupied genes, using existing CREB1
163 ChIP-seq data from A549 and HepG2 cells (Figure 3C, Supplementary table 2). We observed
164 that 51 genes were found in both the A549 and HepG2 datasets. From the 51 candidates, we
165 noticed a lncRNA gene, CCAT1, that had previously been demonstrated to be important in
166 several stages of CRC, especially in relation to cell proliferation (Figure 3D and 3E) (Kim et al.,
167 2015). Moreover, MYC, which was positively regulated by CCAT1-L via its role in recruitment
168 of CTCF in HCT116, was obviously downregulated in KO-CREB1 cells (Figure 3D and 3F)
169 (Xiang et al., 2014). The promoter of E2F1 was also shown to be occupied by CREB1 in all
170 four ChIP-seq datasets despite the absence of E2F1 in the downregulated genes from the
171 RNA-seq experiments (Figure 3G). Additionally, CREB1 was found to have the potential to
172 promote the transcription of MYC in light of CREB1 ChIP-seq (Supplementary figure 2A). Thus,
173 these data suggest that CREB1 is involved in the transactivation of CCAT1 lncRNA and
174 transcriptional regulatory proteins.

175 To test the above results and assumptions, rescue experiments were first performed, and
176 the results showed that CREB1 overexpression in HCT116 cells and restoration in KO-CREB1
177 cells remarkably enhanced the expression of CCAT1, but it significantly increased MYC and
178 E2F1 only in KO-CREB1 cells (Figure 3H and 3I). Then, we subcloned the CREB1 binding sites
179 (CBSs) in CCAT1 (named CCAT1-CBS1 and CCAT1-CBS2) into pGL4.27, which contains a
180 minimal promoter. E2F1-CBS1, which already contains the promoter of E2F1, was subcloned
181 into the promoterless vector pGL4.11. The constructs were cotransfected into HCT116 cells

182 with pcDNA3-CREB1. As expected, the CBS fragments responded to CREB1 in a dose-
183 dependent manner (Figure 3J). Third, we performed a ChIP assay with HCT116 cells using an
184 antibody against CREB1 and observed an enrichment of CCAT1 and E2F1 promoter fragments
185 containing the CBS region over that of the normal IgG, which served as a nonspecific control
186 (Figure 3K). In contrast, CREB1 did not occupy on the promoter of MYC in HCT116 cells
187 (Supplementary figure 2B). Taken together, these results indicate that CCAT1 and E2F1, but
188 not MYC, are transcribed by CREB1.

189 To further clarify the effect of dysregulation of CCAT1 on MYC, we performed *in cis*
190 overexpression and downregulation of CCAT1-L in HCT116 cells based on CRISPRa and
191 CRISPRi, respectively. Compared to the control, the overexpression of CCAT1-L indeed
192 enhanced MYC expression (Figure 3L). Consistently, the downregulation of CCAT1-L reduced
193 the expression of MYC (Figure 3L). Previous studies have shown that MYC acts as a
194 transcriptional activator of E2F1 and CCAT1, but it acts as a repressor to CDKN1A, CDKN1B
195 and CDKN2B. Then, we conducted MYC overexpression and knockdown assays to explore its
196 role in these genes. As a result, MYC negatively regulated the expression of CDKN1A,
197 CDKN1B and CDKN2B, but it did not alter E2F1 and CCAT1 (Supplementary figure 2C-F).
198 These data suggest that CREB1 influences the expression of CCAT1, MYC and E2F1. Then,
199 the downregulation of MYC was found to increase the expression of growth-arresting genes
200 CDKN1A, CDKN1B and CDKN2B.

201 In summary, these results reveal that CREB1 depletion negatively impacts cell proliferation
202 and G1/S transition by directly downregulating the transcription of the lncRNA CCAT1 and the
203 transcription factor E2F1.

204

205 **Increasing the migration and invasion by CREB1-deficiency depends on NF-κB pathway**
206 **activation**

207 To explore the mechanism by which CREB1-deficiency contributes to increased cell migration
208 and invasion, we measured the expression of EMT markers in wild-type and KO-CREB1
209 HCT116 cells. As shown in Figure 4A and 4B, knockout of CREB1 in HCT116 cells enhanced
210 the expression of ZEB1, Vimentin, VIM-AS1 and Slug and concomitantly decreased E-cadherin
211 levels (Boque-Sastre et al., 2015). Conversely, CREB1 overexpression in HCT116 cells and its

212 restoration in KO-CREB1 cells increased the expression of E-cadherin and reduced Vimentin
213 and Slug (Supplementary figure 4A).
214 Our 45-pathway reporter assays revealed that the NF-κB signaling pathway, which is
215 essential for EMT (Huber et al., 2004), was significantly upregulated in KO-CREB1 HCT116
216 cells. By qPCR analysis, the mRNA levels of the NF-κB signaling target genes BCL2A1, IL-8,
217 and CXCL-1 were also significantly upregulated by the loss of CREB1 in HCT116 cells (Figure
218 4C) (Zong et al., 1999, Kunsch et al., 1994, Wood et al., 1995) . The re-expression of CREB1
219 in KO-CREB1 cells reversed the induction of NF-κB signaling pathway (Figure 4D).
220 To further investigate whether the NF-κB signaling pathway is closely involved in CREB1
221 knockout-induced EMT, we used IKK-2 inhibitor IV, a selective inhibitor of the NF-κB signaling
222 pathway, to repress its activity in HCT116 and KO-CREB1 cells. The NF-κB signaling reporter
223 assay and the expression profile of its target genes confirmed the inhibition of the pathway in
224 both HCT116 wild-type and KO-CREB1 cells (Supplementary figure 3B and 3C). Next, EMT
225 markers were analysed by qPCR and Western blot in HCT116 and KO-CREB1 cells treated
226 with 10 μM IKK-2 inhibitor IV for 6 h. As shown in Figure 4E and 4F, IKK-2 inhibitor IV treatment
227 increased the expression of E-cadherin but decreased the levels of the mesenchymal marker.
228 Consistently, inhibition of NF-κB pathway activity with IKK-2 inhibitor IV decreased the migration
229 and invasion ability of HCT116 and KO-CREB1 cells (Figure 4G). Taken together, these results
230 suggest that the NF-κB pathway promotes the EMT that is induced by CREB1 knockout in
231 HCT116 cells.
232 Previous data suggest that the activity of the NF-κB pathway is positively correlated with
233 the phosphorylation of p65; thus, the augmentation of the NF-κB pathway may be due to the
234 increasing level of phosphorylation of p65 (Perkins and Gilmore, 2006). We then detected the
235 protein levels of total and phosphorylated p65 as well as the expression of IKKa, IKKb and IkBa
236 in wild-type and KO-CREB1 HCT116 cells. However, no obvious changes in the expression
237 levels of these proteins were observed (Supplementary figure 3D). Thus, we hypothesized that
238 other factors, such as CREB-binding protein (CBP) and its paralog p300, have a modulating
239 role in the NF-κB signaling pathway independent of inducible nuclear translocation and
240 posttranslational modifications (Gerritsen et al., 1997). To test this hypothesis, we detected the
241 occupancy of CBP/p300 at the p65 binding site in the promoter of Slug and Vimentin with ChIP

242 experiments for CBP and p300 in wild-type and KO-CREB1 HCT116 cells (Choi et al., 2015,
243 Boque-Sastre et al., 2015, Chua et al., 2006). As shown in Figure 4H and Supplementary figure
244 3E, binding of CBP/p300 following CREB1 knockout was specifically enriched in the promoter
245 of EMT markers (Slug and Vimentin) and the NF-κB signaling pathway target gene IL-8,
246 indicating mutual competition of transcriptional coactivators between the two pathways.
247 Collectively, these experiments demonstrate that disruption of CREB1 releases CBP/p300,
248 leading to the activation of the NF-κB signaling pathway and consequent transcription of EMT-
249 associated genes, revealing a previously unknown mechanism for pathway activation mediated
250 by CREB1 depletion.
251
252 **Discussion**
253 High levels of CREB have been observed presented in many kinds of tumours, and it correlates
254 with a high risk of tumorigenesis and a poor clinical outcome (Wu et al., 2007, Chhabra et al.,
255 2007, Bulun et al., 2009, Shankar et al., 2005, Shankar and Sakamoto, 2004). In this report,
256 we demonstrate that knockout of CREB1 impedes cell proliferation resulting in dysregulation of
257 the G1/S phase transition, which is driven, at least in part, by the transcriptional downregulation
258 of the lncRNA CCAT1 and of E2F1 (Figure 5, upper panel). However, We also observed
259 increased cell migration and invasion in the setting of CREB1-deficiency, and this was probably
260 due to the induction of EMT via NF-κB pathway activation (Figure 5, lower panel). Thus, our
261 findings provide a mechanism underlying CREB1 contributes to tumour cell plasticity, which
262 leads to a better understanding of the complexity of the CREB1 function and regulatory network.
263 Given this complexity, we sought direct experimental demonstration that CREB1 can
264 indeed promote cell proliferation as well as inhibit metastasis. Using CREB1 knockout cells, re-
265 expression of CREB1 remarkably reduce the metastatic properties (Figure 1J and 1K). At the
266 same time, exogenous CREB1 could increase proliferation in CREB1-deficency cells.
267 Nevertheless, the proliferation of wild-type cells was unresponsive to the overexpression of
268 CREB1, we reported previously that the metastatic ability of the cells was greatly reduced upon
269 forced expression of CREB1 (Guo et al., 2016b). In addition, the regulation of MYC by
270 CREB1/CCAT1 axis did not contribute to the expression of ITGB and ITGAV, which are involved
271 in the motility and invasiveness of breast cancer cells (Supplementary figure 3F) (Hong et al.,

272 2012). Thus, the opposite role of oncogenes that can promote proliferation pathways but
273 simultaneously suppress migration pathways might be an intrinsic mechanism of cancer cell
274 plasticity in tumours, although more examples need to be uncovered.

275 In this study, the lncRNA CCAT1 and the cell cycle-associated transcription factor E2F1
276 were validated as a novel ncRNA target and protein target of CREB1, respectively. It is worth
277 noting that CCAT1, which was identified as an upregulated lncRNA in CRC, was associated
278 with the malignant progression of CRC, involving cell proliferation, invasion and migration *in*
279 *vitro* and *in vivo* (Nissan et al., 2012, Kam et al., 2013, Xin et al., 2016). Although
280 overexpression of CREB1 in HCT116 cells can promote the expression of CCAT1, as well as
281 CCAT1-L, by approximately 2-fold, the restoration of CREB1 in HCT116 KO-CREB1 cells can
282 increase CCAT1 levels, approaching but not exceeding its expression in HCT116 cells with wild-
283 type CREB1 (Figure 3H). In addition, the expression of E2F1 was not changed significantly in
284 HCT116 cells with forced expression of CREB1. Thus, CREB1 may only contribute to basal
285 transcription of CCAT1 and E2F1, and it may maintain cell proliferation through basal control of
286 the cell cycle, especially in the G1/S phase transition. Additionally, CREB1 has been reported
287 to regulate the cell cycle by transactivation of its downstream genes, including CCND1, CCNE1,
288 CCNA1 and CCNA2, while the expression of CCND1 and CCNE1 did not change significantly
289 in the RNA or protein level in CREB1-knockout HCT116 cells. The CREB1 occupancy of the
290 CRE motif in the CCND1 and CCNE1 genes was validated with ChIP-PCR, suggesting a direct
291 role for CREB1 in regulation CCND1 and CCNE1 in HCT116 cells (Supplementary figure 3H).
292 By studying genomic sequences, the complex promoter of the CCND1 and CCNE1 genes were
293 found to contain many transcription factor binding sites that may control their transcriptions
294 depending on the particular cellular or functional context (data not shown). Therefore, the
295 absence of CREB1 in HCT116 cells might be compensated for by other genes.

296 Our finding that CREB1 overexpression leads to inhibition of cell migration and invasion
297 through suppression of the NF-κB pathway supports notion that the NF-κB pathway function in
298 angiogenesis, invasion and metastasis (Chua et al., 2006, Huang et al., 2001, Huber et al.,
299 2004). However, none of previous reports has linked the effect of CREB1 on NF-κB pathway
300 activity to cell motility and invasiveness, and none has implicated the EMT markers in the
301 cellular changes elicited by CREB1. Our results demonstrate that the disruption of CREB1

leads to a loss of its ability to compete with p65 for limiting amounts of coactivators CBP/p300, which in turn increases properties that are essential for metastasis. These data, however, do not mean that CREB1 affects invasion and metastasis only through regulation of the NF-κB pathway-mediated EMT. The fact that CREB1 has been reported to induce the expression of MMP-2/9 and proteins associated with EMT in Renal cell carcinoma (Wang et al., 2017). Nevertheless, as inhibition of the NF-κB pathway activity by IKK-2 inhibitor IV is sufficient to counteract the repressive effect of CREB1 in migration and invasion, it is apparent that a primary effect of CREB1 on motility in HCT116 cells is mediated through its inhibition of the NF-κB pathway.

Ultimately, the findings reported here raise the possibility that inhibition of CREB1 in human tumours might at times be contraindicated because its suppression may indeed promote metastasis and therefore, inhibition of the NF-κB pathways should be taken into consideration as a combinatorial treatment in therapeutic strategies involving CREB1.

Materials and methods

Key resources table

Reagent type (species) or resource	Designation	Source or reference	Identifiers	Additional information
Cell line (Homo sapiens)	HCT116	the Shanghai Institute of Cell biology, Chinese Academy of Science	TCHu 99	
Cell line (Homo sapiens)	HEK293T	the Shanghai Institute of Cell biology, Chinese Academy of Science	GNHu17	
Chemical compound, drug	IKK-2 inhibitor IV	Calbiochem	Cat# 401484	Working concentration: 10μM
Chemical compound, drug	Puromycin	Meilune	Cat# MB2005	Working concentration:3 μg/mL
Chemical compound, drug	Blasticidin	Meilune	Cat# MB2506	Working concentration:10 μg/mL
Commercial assay, kit	Cignal 45-pathway reporter arrays	QIAGEN	Cat# C82DB0D7-3D10-4B	

Commercial assay, kit	Dual-Luciferase Reporter Assay Systems	Promega	Cat# E1910
Commercial assay, kit	Calcein-AM/PI Double Stain Kit	Yeasen	Cat# 40747ES76
Commercial assay, kit	Cell Counting Kit-8	Dojindo Molecular Technologies	Cat# CK04-20
Commercial assay, kit	Propidium iodide (PI) Kit	MultiSciences	Cat# 70-CCS012
Antibody	CREB1	Cell Signaling Technology	Cat# 9197S
Antibody	p300	Cell Signaling Technology	Cat# 7425
Antibody	CBP	Santa Cruz Biotechnology	Cat# sc-584
Antibody	Normal Rabbit IgG	Cell Signaling Technology	Cat# 2729
Antibody	MYC	Cell Signaling Technology	Cat# 9402
Antibody	E2F1	Cell Signaling Technology	Cat# 9402
Antibody	p15	Cell Signaling Technology	Cat# 4822
Antibody	p21	Cell Signaling Technology	Cat# 2946
Antibody	p27	Cell Signaling Technology	Cat# 2552
Antibody	Cyclin D1	Cell Signaling Technology	Cat# 2926
Antibody	Cyclin E1	Cell Signaling Technology	Cat# 4129
Antibody	E-cadherin	Cell Signaling Technology	Cat# 3195
Antibody	Vimentin	Cell Signaling Technology	Cat# 5741
Antibody	Slug	Cell Signaling Technology	Cat# 9585
Antibody	NF-κB Pathway Sampler Kit	Cell Signaling Technology	Cat# 9936
Antibody	GAPDH	Cell Signaling Technology	Cat# 2118
Recombinant DNA reagent	lenti dCAS-KRAB_Blast	This paper	
Vector	PX462	Addgene	Cat# 48141
Vector	lenti dCAS-VP64_Blast	Addgene	Cat# 61425
Vector	psPAX2	Addgene	Cat# 12260
Vector	pMD2.G	Addgene	Cat# 12259
Vector	pLKO.1-TRC	Addgene	Cat# 10878
Vector	pGL4.11	Promega	Cat# E6661
Vector	pGL4.27	Promega	Cat# E8451
Sequence-based reagent	pLKO-shLacZ	This paper	
Sequence-based reagent	pLKO-shMYC	This paper	
Sequence-based reagent	Oligonucleotides for vectors	This paper	Supplementary table 3

	construction and T7E1 assay			
Sequence-based reagent	Oligonucleotides for qPCR analysis	This paper	Supplementary table 4	
Sequence-based reagent	Oligonucleotides for ChIP PCR	This paper	Supplementary table 5	
Software, algorithm	Image-Pro Plus			Used for transwell and CFA assays quantification
Software, algorithm	FlowJo_v7			Used for Flow cytometry data quantification and visualization
Software, algorithm	Integrative Genomics Viewer (IGV_2.8.0)			Used for ChIP-seq data visualization
Software, algorithm	GSEA (v4.0.2)			
Software, algorithm	STAR (v2.4.2a)			
Software, algorithm	RSEM (v1.2.28)			
Software, algorithm	GraphPad Prism (v6.0.0)			

Cell cultures and treatments

The human colon cancer cell line HCT116 and human embryonic kidney cell line HEK293T were obtained from the Shanghai Institute of Cell biology, Chinese Academy of Science. Cell lines were maintained using standard media and conditions. To inhibit the NF-κB pathway, HCT116 and KO-CREB1 cells were treated with different concentrations of 5, 10, 15 and 20 μM IKK-2 inhibitor IV (Calbiochem, #401484) for 6 hr in a serum-free medium, and DMSO (Sigma) was used as a control.

Cell transfection

Transfection of plasmid DNA was performed using Lipofectamine LTX reagent or Lipofectamine 2000 (Invitrogen), and all RNA transfections were performed at a final concentration of 50 nM

330 using Lipofectamine 2000 (Invitrogen) according to the manufacturer's instruction. Besides,
331 Cignal 45-pathway reporter arrays plasmids were transfected with ViaFect™ Transfection
332 Reagent (Promega).
333
334 **Knockout of CREB1**
335 The CRISPR/Cas9 Nickase (CRISPR/nCas9) system was used to construct the HCT116 KO-
336 CREB1 cells (Guo et al., 2016a). The HCT116 cells were transfected with PX462-C1C2 using
337 Lipofectamine 2000 and cultured in the presence of puromycin (3 μg/mL, Sigma) for 48 hr after
338 post-transfection 24 hr. Single-cells clones were generated by dilution assays and tested for
339 knockout of CREB1 expression by Western blot.
340
341 **RNA-seq sequencing and analysis**
342 RNA-sequencing was performed by RiboBio Co., Ltd. Briefly, ribosomal RNA was depleted from
343 HCT116 wild-type and KO-CREB1 cells by using a Ribo-Zero rRNA Removal Kit (Epicentre).
344 Then, the RNA was used as input for the Illumina TruSeq® Stranded Total RNA HT/LT Sample
345 Prep Kit (Illumina). Libraries were pooled and sequenced on an Illumina Hiseq 3000 PE150
346 platform. A minimum of 50 M reads were generated per sample. RNA-sequencing reads were
347 trimmed for adaptor sequence and mapped to the GENCODE V19 using STAR and RSEM.
348 Then, protein coding genes exhibiting differential expression with PPDE>0.95 were included in
349 Gene Ontology and Protein-protein Interaction analyses using Metascape (Tripathi et al., 2015).
350 For GSEA, the cAMP signaling pathway gene set was generated according to the gene list from
351 KEGG; then normalized expression data were analyzed and visualized with GSEA software
352 (version 3.0, http://www.broadinstitute.org/gsea/) (Subramanian et al., 2005, Kanehisa et al.,
353 2018).
354
355 **ChIP-seq Data analysis and visualization**
356 Both RNA polymerase II and CREB1 ChIP-seq data were previously published and were
357 obtained from NCBI GEO accession numbers: GSM935426(HCT116, RNA polymerase II),
358 GSM1010808(HepG2, CREB1) and GSM1010719(A549, CREB1). Peaks were identified using
359 MACS2 with default parameters (Feng et al., 2012). All data were visualized using Integrative

360 Genomics Viewer (IGV) software.

361

362 **Vectors construction**

363 The pcDNA3 vector (Invitrogen) was used for generation CREB1 and MYC expression vectors.
364 CBS1 and CBS2 of CCAT1 and E2F1-CBS upstream of E2F1 were amplified from HCT116
365 genome and inserted into pGL4.27 and pGL4.11 (Promega) in the sense orientation relative to
366 the luciferase coding sequence, respectively. For stable expression of dCas9-KRAB, the lenti
367 dCAS-KRAB_Blast vector was modified from lenti dCAS-VP64_Blast vector (Addgene) as
368 follows: the KRAB domain (from ZNF10) was amplified by PCR from HEK293T cDNA and
369 cloned into lenti dCAS-VP64_Blast vector using *Bam*HI and *Bsp*1407I double digestion by
370 ClonExpress MultiS kit (Vazyme). For transient expression of sgRNA, the pU6-sgRNA vectors
371 was constructed by subcloning the U6 promoter-sgRNA scaffold from PX462 (Addgene) to
372 pMD-18T vector (Takara). The sgRNA expression plasmids were cloned by insert annealed
373 oligos into the pU6-sgRNA vector that was digested by *Bbs* I (NEB). shRNA for *Lac*Z (negative
374 control) and MYC were generate according to the pLKO.1 protocol from Addgene. Cignal 45-
375 pathway reporter arrays, the CREB pathway reporter and the NF-κB pathway reporter that
376 measure the activity of the corresponding pathway were purchased from Qiagen. The primers
377 used for vector construction are listed in Supplementary table 3.

378

379 **Genomic DNA extraction, amplification and T7E1 assay**

380 Genomic DNA (gDNA) from HCT116 single-cells clones, which transfected with sgRNAs
381 targeted CREB1 were extracted with Hipure Tissue DNA mini kit (Magen) according to the
382 manufacturer's instruction. Then, the target region was amplified by Phusion® High-
383 Fidelity DNA Polymerase (NEB), and the indel of the sgRNAs was assessed by the T7
384 endonuclease I assay (Viewsolid Biotech). The primers used for T7E1 assay are listed in
385 Supplementary table 3.

386

387 **Lentiviral Transduction for Stable cell lines**

388 The lenti dCAS-VP64_Blast, lenti dCAS-KRAB_Blast, pLKO-shLacZ or pLKO-shMYC vectors
389 were co-transcripted with packaging vectors psPAX2 and pMD2.G into HEK293T cells for

390 lentivirus production. To establish stable cell lines, HCT116 cells were transduced by using the
391 above lentiviral particles with polybrene (6 μg/mL, Sigma). After 24 hr, the infected cells were
392 subjected to selection in medium containing blasticidin (10 μg/ml, Meilune) or puromycin (3
393 μg/ml, Meilune) for 5 days.
394
395 **RNA extraction and qPCR assays**
396 Total RNA was extracted from HCT116 wild-type and KO-CREB1 cells with TRIzol reagent
397 (Invitrogen) according to the manufacturer's instruction. and then reverse-transcribed to cDNA
398 using the primescript™ RT reagent kit (Takara). Real-time PCR was carried out using SYBR
399 Premix ExTaq™ (Takara) according to manufacturer's instructions. GAPDH were employed as
400 endogenous controls. The comparative Ct Method (ΔΔCT Method) was used to determine the
401 expression levels of genes. All primer sets were purchased from Synbio Technologies (Suzhou,
402 China), and the primer sequence used for qRT-PCR are show in Supplementary table 4.
403
404 **Cell viability assay**
405 Cell viability was measured using Cell Counting Kit-8 (CCK-8, Dojindo Molecular Technologies).
406 HCT116, KO-CREB1 and 24 hr post-transfection cells were seeded into a 96-well plate at 2×10^3
407 cells per well. Then evaluating cell viability with CCK-8 at the time of 24, 48, 72, 96, 120 hr. The
408 detected wavelength 450 nm, and the reference wavelength 630 nm were measured after
409 incubation for 2 hr at 37℃.
410
411 **Calcein-AM/PI double staining**
412 Calcein-AM/PI double staining of wild-type and KO-CREB1 HCT116 cells were performed
413 according to the manufacturer's instruction (Calcein-AM/PI Double Stain Kit, Yeasen). Brife,
414 cells incubated in 1×Assay Buffer containing 0.67 μM Calcein-AM and 1.5 μM propidiumiodide
415 (PI) at 37 °C for 15 min. After washing with PBS, cells were viewed in a fluorescence microscopy.
416 The cells were counted using a Image Pro-Plus software.
417
418 **Cell cycle analysis**
419 Cell cycle distribution was assessed by flow cytometry using Propidium iodide (PI) Kit

420 (MultiSciences). HCT116, KO-CREB1 and 24 hr post-transfection cells were treated with
421 vehicle or Nocodazole for 24 hr. Then the cells were resuspended in trypsin and centrifuged at
422 400 × g for 3 min at room temperature. The cell pellet was washed once by PBS and
423 resuspended in 1 ml reagent A and in 10 μl reagent B. After incubating for 30 min at room
424 temperature, the cell cycle was examined by flow cytometry.
425
426 **Colony formation assay**
427 For evaluating effect of CREB1 knockdown on clonogenicity, cells were plated into 6-well plates
428 with 2×10^3 cells per well. After one week, colonies (>50 cells per colony) were fixed and stained
429 with crystal violet in methanol. The colonies were counted using a Image Pro-Plus software.
430
431 **Luciferase reporter assays**
432 Both forward and reverse transfection methods have been applied for luciferase reporter assay.
433 And 45-pathway assay is performed with reverse transfection, forward transfection is employed
434 for promoter assay, and pathway assay. For forward transfection, cells are plated in 48-well
435 plate 24 hr before transfection. 48 hr post-transfection, cell extracts were assayed for luciferase
436 activity using the Dual-Luciferase Reporter Assay Systems (Promega) according to the
437 manufacturer's instruction. Reverse transfection involves plating cells into the transfection
438 complexes in a one day procedure. For promoter assay and 45-pathway assay, the Renilla
439 luciferase was used as a control to normalize luminescence levels.
440
441 **Migration and invasion assays**
442 For HCT116 and KO-CREB1 migration and invasion assay, the cells were suspended in 200 μl
443 medium without FBS, and then were seeded into upper chamber of transwell inserts (8 μM pore
444 size, Costar) with or without coated Matrigel (R&D System). The lower chamber of the transwell
445 was filled with 750 μl medium supplemented with 10% FBS which function as a chemoattractant.
446 After 24 hr incubation in 37℃, cells that migrated or invaded to the lower surface of the insert
447 membrane were fixed in methanol and stained by 0.1% crystal violet. For IKK-2 Inhibitor IV
448 treated cells migration and invasion assay, the cells were treated with 10 μM IKK-2 Inhibitor IV
449 for 6 hr after 48 hr post-seeding. Then the cells were placed into the upper chamber with the

450 non-coated or Matrigel-coated membrane, which was diluted with 200 μl serum-free culture
451 medium. After the cells were incubated for 24 hr at 37°C in a humidified incubator, the cells
452 adhering to the lower surface were fixed in methanol and stained by 0.1% crystal violet. The
453 numbers of cells that have migrated or invaded were captured under Zeiss AxioObserver.Z1
454 (Carl Zeiss) at a magnification of 50×. And cell counting was processed by Image Pro-Plus
455 software.
456
457 **Western blot analysis**
458 Total protein was extracted using either TRIzol reagent (Invitrogen) as recommended or RIPA
459 buffer (50mM Tris-HCl,pH 7.4, 150mM NaCl, 0.1% SDS, 1% Sodium deoxycholate, 1% Triton
460 X-100, 2mM EDTA and 1×Protease Inhibitor Cocktail). Protein precipitation isolated by TRIzol
461 was lysed in the buffer containing 1% DTT, 4% CHAPS, 7 M urea, 2 M thiourea and 2%
462 ampholine. Equal total protein extracts were loaded and separated by SDS-polyacrylamide gel
463 electrophoresis (SDS-PAGE), transferred onto Protran™ nitrocellulose membranes (Whatman).
464 The following antibodies were used for western blot: CREB1 (CST, 9197S), MYC(CST, 9402S),
465 E2F1(CST, 9402S), p15(CST,4822S), p21(CST, 2946S), p27(CST, 2552S), Cyclin D1(CST,
466 2926S), Cyclin E1(CST, 4129S), E-cadherin (CST, 3195S), Vimentin (CST, 5741S), Slug(CST,
467 9585), NF-κB Pathway Sampler Kit (CST, 9936) or GAPDH (CST, 2118S). GAPDH was used
468 as the loading control.
469
470 **ChIP assay**
471 HCT116 cells were cross-linked with 1% formaldehyde (Sigma) in new culture medium for 10
472 min and the reaction quenched with addition of glycine to a final concentration of 0.125 M at
473 room temperature for 5 min. Cells were rinsed with cold PBS twice and scraped from the dishes.
474 Pellet cells were resuspended in cell lysis buffer (20mM Tris-HCl at pH 8.0, 85 mM KCl, and
475 0.5% NP-40) and incubated on ice for 15 min, vortexing the cell suspension briefly every 5 min
476 to facilitate the release of the nuclei. Nuclear lysis buffer (10mM Tris-HCl at pH 7.5, 1% NP40,
477 0.5% deoxycholate and 0.1% SDS) containing protease inhibitor mixture (Complete Mini tablets,
478 Roche Diagnostics) was used to lyse the nuclei at a concentration of 1×107 cells/ml. After
479 sonication, the chromatin lysates were divided into 500 μl aliquots. Each 500 μl sonicated

480 chromatin (1×106 cells) pre-cleared with 10 μl Protein G Magnetic bead (Invitrogen). 5 μl (1%)
481 of the supernatant was reserved as Input. Cleared samples were immunoprecipitated over-
482 night in IP buffer with 10 μL of CREB1 (CST, 9197S), 10 μL of CBP (CST, 7425S), 10uL of p300
483 (Santa Cruz, sc-584) or 2μL negative control antibody rabbit IgG (CST, 2729). Immune
484 complexes were successively washed twice with Low Salt Wash Buffer (0.1% SDS, 1% Trition
485 X 100, 2mM EDTA, 20mM Tris-HCl (pH 8.0), 150mM NaCl) , twice with High Salt Wash Buffer
486 (0.1% SDS, 1% Trition X 100, 2mM EDTA, 20mM Tris-HCl (pH 8.0), 500mM NaCl), twice with
487 LiCl Wash Buffer (0.25M LiCl, 1% NP-40, 1% deoxycholate, 1mM EDTA and 10mM Tris-HCl
488 (pH 8.0)) and twice with TE Buffer (10mM Tris-HCl (pH 8.0) and 1mM EDTA) for 3 min. The
489 precipitated chromatin was eluted and reversed cross-linked in ChIP Elution Buffer (1% SDS
490 and 0.1M $NaHCO_3$) containing proteinase K and RNase A two hours at 65 °C. The DNA was
491 recovered and purified using Qiagen PCR purification kit. The semi-quantitative PCR or qPCR
492 was performed to analyse the immunoprecipitated DNA. Primers are listed in Supplementary
493 table 5.
494
495 **Statistical Analysis**
496 Quantitative data were presented as the mean ± the standard error of the mean (SEM) from a
497 minimum of three independent experiments. Comparisons between two groups were analyzed
498 using the Student's *t*-tests with n=3, unless otherwise indicated. Statistical analyses were
499 performed with GraphPad Prism 6 (GraphPad Software Inc.). $p<0.05$ was considered to be
500 statistically significant.
501
502 **Additional information**
503 **Competing interests**
504 The authors declare no conflict of interest.
505
506 **Funding**
507 This work was supported by the National Natural Science Foundation of China (31970604,
508 31900903, 31671349, 31770879); and the National Key R&D Program of China
509 (2017YFA0504400). This research was supported in part by the Guangdong Province Key

Laboratory of Computational Science (13lgjc05) and the Guangdong Province Computational Science Innovative Research Team (14lgjc18).

Author contributions

L.H.Q., J.H.Y., H.Z. and B.L. conceived and designed the entire project. L.H.Q., J.H.Y. and H.Z. supervised the research. B.L., L.S.Z., C.M.Z., Q.J.H., Y.H.G., L.Q.W., P.Y., S.R.L., Q.L., Y.X.L. and J.H.Y. performed the experiments and/or data analyses. B.L. performed the genome-wide or transcriptome-wide data analyses. B.L., L.H.Q. and J.H.Y. contributed reagents/analytic tools and/or grant support. B.L., L.S.Z., C.M.Z., Q.J.H., Y.H.G., L.Q.W., P.Y., S.R.L., Q.L., Y.X.L., H.Z., J.H.Y. and L.H.Q. wrote and revised the paper. All authors discussed the results and commented on the manuscript.

Acknowledgments

pSpCas9n(BB)-2A-Puro (PX462) was a gift from Feng Zhang (Addgene plasmid #48141). lenti dCAS-VP64_Blast was a gift from Feng Zhang (Addgene plasmid #61425). pLKO.1-TRC cloning vector was a gift from David Root (Addgene plasmid #10878). psPAX2 was a gift from Didier Trono (Addgene plasmid #12260). pMD2.G was a gift from Didier Trono (Addgene plasmid #12259).

Additional files

Supplementary figure 1. Knockout of CREB1 in HCT116 cells.

Supplementary figure 2. CREB1 facilitates the G1/S transition by transactivating of CCAT1 and E2F1.

Supplementary figure 3. Increases in the migration and invasion of KO-CREB1 cells are due to the induction of EMT via activation of the NF-κB pathway.

Supplementary table 1. Genes differentially expressed upon knocking out of CREB1 in HCT116 cells identified by the RNA-seq analysis.

Supplementary table 2. The gene lists used for comparing ChIP-seq and RNA-seq.

Supplementary table 3. Primers used for vectors construction andT7E1 assay.

Supplementary table 4. Primers used for reverse transcription and real-time PCR

540 **Supplementary table 5**. Primers used for ChIP PCR

541

542

Reference

BERKOWITZ, L. A., RIABOWOL, K. T. & GILMAN, M. Z. 1989. Multiple sequence elements of a single functional class are required for cyclic AMP responsiveness of the mouse c-fos promoter. *Mol Cell Biol,* 9**,** 4272-81.

BIAN, Z., JIN, L., ZHANG, J., YIN, Y., QUAN, C., HU, Y., FENG, Y., LIU, H., FEI, B., MAO, Y., ZHOU, L., QI, X., HUANG, S., HUA, D., XING, C. & HUANG, Z. 2016. LncRNA-UCA1 enhances cell proliferation and 5-fluorouracil resistance in colorectal cancer by inhibiting miR-204-5p. *Sci Rep,* 6**,** 23892.

BOQUE-SASTRE, R., SOLER, M., OLIVEIRA-MATEOS, C., PORTELA, A., MOUTINHO, C., SAYOLS, S., VILLANUEVA, A., ESTELLER, M. & GUIL, S. 2015. Head-to-head antisense transcription and R-loop formation promotes transcriptional activation. *Proc Natl Acad Sci U S A,* 112**,** 5785-90.

BOULON, S., DANTONEL, J.-C. C., BINET, V., VIé, A., BLANCHARD, J.-M. M., HIPSKIND, R. A. & PHILIPS, A. 2002. Oct-1 potentiates CREB-driven cyclin D1 promoter activation via a phospho-CREB- and CREB binding protein-independent mechanism. *Molecular and cellular biology,* 22**,** 7769-7779.

BULUN, S. E., LIN, Z., ZHAO, H., LU, M., AMIN, S., REIERSTAD, S. & CHEN, D. 2009. Regulation of aromatase expression in breast cancer tissue. *Ann N Y Acad Sci,* 1155**,** 121-31.

CARLEZON, W. A., JR., DUMAN, R. S. & NESTLER, E. J. 2005. The many faces of CREB. *Trends Neurosci,* 28**,** 436-45.

CHHABRA, A., FERNANDO, H., WATKINS, G., MANSEL, R. E. & JIANG, W. G. 2007. Expression of transcription factor CREB1 in human breast cancer and its correlation with prognosis. *Oncol Rep,* 18**,** 953-8.

CHOI, M. J., CHO, K. H., LEE, S., BAE, Y. J., JEONG, K. J., RHA, S. Y., CHOI, E. J., PARK, J. H., KIM, J. M., LEE, J. S., MILLS, G. B. & LEE, H. Y. 2015. hTERT mediates norepinephrine-induced Slug expression and ovarian cancer aggressiveness. *Oncogene,* 34**,** 3402-12.

CHUA, H. L., BHAT-NAKSHATRI, P., CLARE, S. E., MORIMIYA, A., BADVE, S. & NAKSHATRI, H. 2006. NF-κB represses E-cadherin expression and enhances epithelial to mesenchymal transition of mammary epithelial cells: potential involvement of ZEB-1 and ZEB-2. *Oncogene,* 26**,** 711-724.

D'AMICO, M., HULIT, J., AMANATULLAH, D. F., ZAFONTE, B. T., ALBANESE, C., BOUZAHZAH, B., FU, M., AUGENLICHT, L. H., DONEHOWER, L. A., TAKEMARU, K., MOON, R. T., DAVIS, R., LISANTI, M. P., SHTUTMAN, M., ZHURINSKY, J., BEN-ZE'EV, A., TROUSSARD, A. A., DEDHAR, S. & PESTELL, R. G. 2000. The integrin-linked kinase regulates the cyclin D1 gene through glycogen synthase kinase 3beta and cAMP-responsive element-binding protein-dependent pathways. *J Biol Chem,* 275**,** 32649-57.

FENG, J., LIU, T., QIN, B., ZHANG, Y. & LIU, X. S. 2012. Identifying ChIP-seq enrichment using MACS. *Nature Protocols,* 7**,** 1728-1740.

FUSCO, S., LEONE, L., BARBATI, S. A., SAMENGO, D., PIACENTINI, R., MAULUCCI, G., TOIETTA, G., SPINELLI, M., MCBURNEY, M., PANI, G. & GRASSI, C. 2016. A CREB-Sirt1-Hes1 Circuitry Mediates Neural Stem Cell Response to Glucose Availability. *Cell*

Rep.

GERRITSEN, M. E., WILLIAMS, A. J., NEISH, A. S., MOORE, S., SHI, Y. & COLLINS, T. 1997. CREB-binding protein/p300 are transcriptional coactivators of p65. *Proc Natl Acad Sci U S A,* 94**,** 2927-32.

GHOSH, S., LU, Y. & HU, Y. 2008. A Role of CREB in BRCA1 Constitutive Promoter Activity and Aromatase Basal Expression. *Int J Biomed Sci,* 4**,** 260-265.

GUO, Y. H., WANG, L. Q., LI, B., XU, H., YANG, J. H., ZHENG, L. S., YU, P., ZHOU, A. D., ZHANG, Y., XIE, S. J., LIANG, Z. R., ZHANG, C. M., ZHOU, H. & QU, L. H. 2016a. Wnt/beta-catenin pathway transactivates microRNA-150 that promotes EMT of colorectal cancer cells by suppressing CREB signaling. *Oncotarget*.

GUO, Y. H., WANG, L. Q., LI, B., XU, H., YANG, J. H., ZHENG, L. S., YU, P., ZHOU, A. D., ZHANG, Y., XIE, S. J., LIANG, Z. R., ZHANG, C. M., ZHOU, H. & QU, L. H. 2016b. Wnt/beta-catenin pathway transactivates microRNA-150 that promotes EMT of colorectal cancer cells by suppressing CREB signaling. *Oncotarget,* 7**,** 42513-42526.

HONG, L., DEREK, C. R., DUN, Y., REN, X., EVETTE, S. R., MINA, J. B. & BISHOP, J. M. 2012. MYC suppresses cancer metastasis by direct transcriptional silencing of αv and β3 integrin subunits. *Nature Cell Biology,* 14**,** 567-574.

HUANG, S., PETTAWAY, C. A., UEHARA, H., BUCANA, C. D. & FIDLER, I. J. 2001. Blockade of NF-kappaB activity in human prostate cancer cells is associated with suppression of angiogenesis, invasion, and metastasis. *Oncogene,* 20**,** 4188-97.

HUBER, M. A., AZOITEI, N., BAUMANN, B., GRUNERT, S., SOMMER, A., PEHAMBERGER, H., KRAUT, N., BEUG, H. & WIRTH, T. 2004. NF-kappaB is essential for epithelial-mesenchymal transition and metastasis in a model of breast cancer progression. *J Clin Invest,* 114**,** 569-81.

HUMMLER, E., COLE, T. J., BLENDY, J. A., GANSS, R., AGUZZI, A., SCHMID, W., BEERMANN, F. & SCHUTZ, G. 1994. Targeted mutation of the CREB gene: compensation within the CREB/ATF family of transcription factors. *Proc Natl Acad Sci U S A,* 91**,** 5647-51.

IMPEY, S., MCCORKLE, S. R., CHA-MOLSTAD, H., DWYER, J. M., YOCHUM, G. S., BOSS, J. M., MCWEENEY, S., DUNN, J. J., MANDEL, G. & GOODMAN, R. H. 2004. Defining the CREB regulon: a genome-wide analysis of transcription factor regulatory regions. *Cell,* 119**,** 1041-54.

JAMES, M. A., LU, Y., LIU, Y., VIKIS, H. G. & YOU, M. 2009. RGS17, an overexpressed gene in human lung and prostate cancer, induces tumor cell proliferation through the cyclic AMP-PKA-CREB pathway. *Cancer Res,* 69**,** 2108-16.

KAM, Y., RUBINSTEIN, A., NAIK, S., DJAVSAROV, I., HALLE, D., ARIEL, I., GURE, A. O., STOJADINOVIC, A., PAN, H., TSIVIN, V., NISSAN, A. & YAVIN, E. 2013. Detection of a long non-coding RNA (CCAT1) in living cells and human adenocarcinoma of colon tissues using FIT-PNA molecular beacons. *Cancer Lett*.

KANEHISA, M., SATO, Y., FURUMICHI, M., MORISHIMA, K. & TANABE, M. 2018. New approach for understanding genome variations in KEGG. *Nucleic Acids Res*.

KIM, T., JEON, Y. J., CUI, R., LEE, J. H., PENG, Y., KIM, S. H., TILI, E., ALDER, H. & CROCE, C. M. 2015. Role of MYC-Regulated Long Noncoding RNAs in Cell Cycle Regulation and Tumorigenesis. *JNCI Journal of the National Cancer Institute,* 107.

KUNSCH, C., LANG, R. K., ROSEN, C. A. & SHANNON, M. F. 1994. Synergistic transcriptional activation of the IL-8 gene by NF-kappa B p65 (RelA) and NF-IL-6. *J Immunol,* 153**,** 153-64.

LEE, H. J., MIGNACCA, R. C. & SAKAMOTO, K. M. 1995. Transcriptional activation of egr-1 by granulocyte-macrophage colony-stimulating factor but not interleukin 3 requires phosphorylation of cAMP response element-binding protein (CREB) on serine 133. *J Biol Chem,* 270**,** 15979-83.

LEE, R. J., ALBANESE, C., STENGER, R. J., WATANABE, G., INGHIRAMI, G., HAINES, G. K., 3RD, WEBSTER, M., MULLER, W. J., BRUGGE, J. S., DAVIS, R. J. & PESTELL, R. G. 1999. pp60(v-src) induction of cyclin D1 requires collaborative interactions between the extracellular signal-regulated kinase, p38, and Jun kinase pathways. A role for cAMP response element-binding protein and activating transcription factor-2 in pp60(v-src) signaling in breast cancer cells. *J Biol Chem,* 274**,** 7341-50.

LEMBERGER, T., PARKITNA, J. R., CHAI, M., SCHUTZ, G. & ENGBLOM, D. 2008. CREB has a context-dependent role in activity-regulated transcription and maintains neuronal cholesterol homeostasis. *FASEB J,* 22**,** 2872-9.

LONZE, B. E. & GINTY, D. D. 2002. Function and regulation of CREB family transcription factors in the nervous system. *Neuron,* 35**,** 605-23.

MICHAEL, M. D., MICHAEL, L. F. & SIMPSON, E. R. 1997. A CRE-like sequence that binds CREB and contributes to cAMP-dependent regulation of the proximal promoter of the human aromatase P450 (CYP19) gene. *Mol Cell Endocrinol,* 134**,** 147-56.

NAGATA, D., SUZUKI, E., NISHIMATSU, H., SATONAKA, H., GOTO, A., OMATA, M. & HIRATA, Y. 2001. Transcriptional activation of the cyclin D1 gene is mediated by multiple cis-elements, including SP1 sites and a cAMP-responsive element in vascular endothelial cells. *J Biol Chem,* 276**,** 662-9.

NISSAN, A., STOJADINOVIC, A., MITRANI-ROSENBAUM, S., HALLE, D., GRINBAUM, R., ROISTACHER, M., BOCHEM, A., DAYANC, B. E., RITTER, G., GOMCELI, I., BOSTANCI, E. B., AKOGLU, M., CHEN, Y. T., OLD, L. J. & GURE, A. O. 2012. Colon cancer associated transcript-1: a novel RNA expressed in malignant and pre-malignant human tissues. *Int J Cancer,* 130**,** 1598-606.

PERKINS, N. D. & GILMORE, T. D. 2006. Good cop, bad cop: the different faces of NF-kappaB. *Cell Death Differ,* 13**,** 759-72.

RAN, F. A., HSU, P. D., LIN, C. Y., GOOTENBERG, J. S., KONERMANN, S., TREVINO, A. E., SCOTT, D. A., INOUE, A., MATOBA, S., ZHANG, Y. & ZHANG, F. 2013. Double nicking by RNA-guided CRISPR Cas9 for enhanced genome editing specificity. *Cell,* 154**,** 1380-9.

RAO, M., ZHU, Y., CONG, X. & LI, Q. 2017. Knockdown of CREB1 inhibits tumor growth of human gastric cancer in vitro and in vivo. *Oncol Rep,* 37**,** 3361-3368.

SHANKAR, D. B., CHENG, J. C., KINJO, K., FEDERMAN, N., MOORE, T. B., GILL, A., RAO, N. P., LANDAW, E. M. & SAKAMOTO, K. M. 2005. The role of CREB as a proto-oncogene in hematopoiesis and in acute myeloid leukemia. *Cancer Cell,* 7**,** 351-62.

SHANKAR, D. B. & SAKAMOTO, K. M. 2004. The role of cyclic-AMP binding protein (CREB) in leukemia cell proliferation and acute leukemias. *Leuk Lymphoma,* 45**,** 265-70.

SUBRAMANIAN, A., TAMAYO, P., MOOTHA, V. K., MUKHERJEE, S., EBERT, B. L., GILLETTE,

M. A., PAULOVICH, A., POMEROY, S. L., GOLUB, T. R., LANDER, E. S. & MESIROV, J. P. 2005. Gene set enrichment analysis: a knowledge-based approach for interpreting genome-wide expression profiles. *Proc Natl Acad Sci U S A,* 102**,** 15545-50.

TAN, X., WANG, S., ZHU, L., WU, C., YIN, B., ZHAO, J., YUAN, J., QIANG, B. & PENG, X. 2012. cAMP response element-binding protein promotes gliomagenesis by modulating the expression of oncogenic microRNA-23a. *Proc Natl Acad Sci U S A,* 109**,** 15805-10.

TRIPATHI, S., POHL, M. O., ZHOU, Y., RODRIGUEZ-FRANDSEN, A., WANG, G., STEIN, D. A., MOULTON, H. M., DEJESUS, P., CHE, J., MULDER, L. C., YANGUEZ, E., ANDENMATTEN, D., PACHE, L., MANICASSAMY, B., ALBRECHT, R. A., GONZALEZ, M. G., NGUYEN, Q., BRASS, A., ELLEDGE, S., WHITE, M., SHAPIRA, S., HACOHEN, N., KARLAS, A., MEYER, T. F., SHALES, M., GATORANO, A., JOHNSON, J. R., JANG, G., JOHNSON, T., VERSCHUEREN, E., SANDERS, D., KROGAN, N., SHAW, M., KONIG, R., STERTZ, S., GARCIA-SASTRE, A. & CHANDA, S. K. 2015. Meta- and Orthogonal Integration of Influenza "OMICs" Data Defines a Role for UBR4 in Virus Budding. *Cell Host Microbe,* 18**,** 723-35.

WANG, J., LIU, X., WU, H., NI, P., GU, Z., QIAO, Y., CHEN, N., SUN, F. & FAN, Q. 2010. CREB up-regulates long non-coding RNA, HULC expression through interaction with microRNA-372 in liver cancer. *Nucleic Acids Res,* 38**,** 5366-83.

WANG, X., CUI, H., LOU, Z., HUANG, S., REN, Y., WANG, P. & WENG, G. 2017. Cyclic AMP responsive element-binding protein induces metastatic renal cell carcinoma by mediating the expression of matrix metallopeptidase-2/9 and proteins associated with epithelial-mesenchymal transition. *Mol Med Rep,* 15**,** 4191-4198.

WILSON, B. E., MOCHON, E. & BOXER, L. M. 1996. Induction of bcl-2 expression by phosphorylated CREB proteins during B-cell activation and rescue from apoptosis. *Mol Cell Biol,* 16**,** 5546-56.

WOOD, L. D., FARMER, A. A. & RICHMOND, A. 1995. HMGI(Y) and Sp1 in addition to NF-kappa B regulate transcription of the MGSA/GRO alpha gene. *Nucleic Acids Res,* 23**,** 4210-9.

WU, D., ZHAU, H. E., HUANG, W. C., IQBAL, S., HABIB, F. K., SARTOR, O., CVITANOVIC, L., MARSHALL, F. F., XU, Z. & CHUNG, L. W. 2007. cAMP-responsive element-binding protein regulates vascular endothelial growth factor expression: implication in human prostate cancer bone metastasis. *Oncogene,* 26**,** 5070-7.

XIANG, J. F., YIN, Q. F., CHEN, T., ZHANG, Y., ZHANG, X. O., WU, Z., ZHANG, S., WANG, H. B., GE, J., LU, X., YANG, L. & CHEN, L. L. 2014. Human colorectal cancer-specific CCAT1-L lncRNA regulates long-range chromatin interactions at the MYC locus. *Cell Res,* 24**,** 513-31.

XIN, Y., LI, Z., SHEN, J., CHAN, M. T. & WU, W. K. K. 2016. CCAT1: a pivotal oncogenic long non-coding RNA in human cancers. *Cell proliferation,* 49**,** 255-260.

YUAN, S., NORGARD, R. J. & STANGER, B. Z. 2019. Cellular Plasticity in Cancer. *Cancer Discov,* 9**,** 837-851.

ZHANG, C., WANG, L., WU, D., CHEN, H., CHEN, Z., THOMAS-AHNER, J. M., ZYNGER, D. L., EECKHOUTE, J., YU, J., LUO, J., BROWN, M., CLINTON, S. K., NEPHEW, K. P., HUANG, T. H., LI, W. & WANG, Q. 2011. Definition of a FoxA1 Cistrome that is crucial for G1 to S-phase cell-cycle transit in castration-resistant prostate cancer. *Cancer Res,*

71**,** 6738-6748.

ZHANG, X., ODOM, D. T., KOO, S. H., CONKRIGHT, M. D., CANETTIERI, G., BEST, J., CHEN, H., JENNER, R., HERBOLSHEIMER, E., JACOBSEN, E., KADAM, S., ECKER, J. R., EMERSON, B., HOGENESCH, J. B., UNTERMAN, T., YOUNG, R. A. & MONTMINY, M. 2005. Genome-wide analysis of cAMP-response element binding protein occupancy, phosphorylation, and target gene activation in human tissues. *Proc Natl Acad Sci U S A,* 102**,** 4459-64.

ZONG, W. X., EDELSTEIN, L. C., CHEN, C., BASH, J. & GéLINAS, C. 1999. The prosurvival Bcl-2 homolog Bfl-1/A1 is a direct transcriptional target of NF-kappaB that blocks TNFalpha-induced apoptosis. *Genes & development,* 13**,** 382-387.

Figure Legends

Figure 1. Effect of knocking out CREB1 on cell proliferation, cell cycle, migration and invasion of HCT116 cells *in vitro*. (A-C) CREB1 pathway reporter assay (A), CREB1 pathway target genes (B), and CREB1 pathway related genes (C) were assessed in CREB1 knockout HCT116 cells; wild-type HCT116 cells were used as vehicle control. (D-E) CCK-8 (D) and colony formation assays (E) showing the effects of CREB1 knockout on the proliferation of HCT116 cells *in vitro*. The quantification of colony formation assays is shown on the right panel. (F-G) Proportions of cells in each phase of the cell cycle were determined by flow cytometry analysis. Both HCT116 and KO-CREB1 cells were treated with DMSO or 100 ng/mL Nocodazole. Quantification of the percentage of cells in each phase of the cell cycle phase was determined for the plots and represented in a graph. (H) CCK-8 assay showing the effect of overexpression on the growth of HCT116 and KO-CREB1 cells. (I) Phase-contrast images of HCT116 and KO-CREB1 cells. (J-K) Restoration of CREB1 expression in KO-CREB1 cells is sufficient to inhibit the migratory and invasive ability of cells. Quantification of the cells was counted for plots and represented in a graph. All experiments were repeated at least three times with similar results. Error bars represent SEM. *$p < 0.05$, as assessed by Student's *t*-tests.

Figure 2. Knocking out CREB1 in HCT116 cells modulates multiple signaling pathways. (A) Volcano map indicating up- or downregulation of genes between wild-type and CREB1 knockout HCT116 cells. (B) GSEA revealing the enrichment of cAMP signaling pathway genes in CREB1 wild-type cells. Genes are ranked by changes in KO-CREB1 cells. (C-E) GO (C and D) and protein-protein interaction (E) analysis of the differentially expressed protein coding genes identified by comparing wild-type and CREB1 knockout HCT116 cells. (F) The 45-pathway assay analysis revealed the effects of CREB1 ablation on the activity of various pathways in HCT116 cells. The data were log2-transformed. All pathway reporter assays and qPCR experiments were performed at least three times. Error bars represent SEM. *$p< 0.05$, as assessed by Student's *t*-tests.

Figure 3. Downregulation of CCAT1 and E2F1 transcription by CREB1 ablation inhibits

cell proliferation and the cell cycle. (A-B) qPCR (A) and Western blot (B) analyses of the expression of genes involved in the G1 phase and G1/S transition in HCT116 and KO-CREB1 cells. GAPDH was used as a loading control. (C) Venn diagram showing the proportion of CREB1-occupied genes whose expression is significantly downregulated in response to knockout of CREB1 in HCT116 cells. (D) qPCR analysis of the expression of CCAT1, CCAT1-L and MYC in HCT116 and KO-CREB1 cells. (E) Schematic representation of the CCAT1, and CCAT1-L (F) gene structures, RNA polymerase II levels of HCT116 cells, and CREB1 levels of HepG2 and K562 cells. (F) Western blot of MYC in HCT116 and KO-CREB1 cells. GAPDH was used as a loading control. (G) Schematic representation of the E2F1 gene structure, RNA polymerase II levels of HCT116 cells, and CREB1 levels in HepG2 and K562 cells. (H) qPCR analysis of CCAT1, CCAT1-L, E2F1 and MYC expression upon introduction of CREB1 in both HCT116 and KO-CREB1 cells. (I) Western blot analysis of E2F1 and MYC protein levels upon introduction of CREB1 in both HCT116 and KO-CREB1 cells. (J) Luciferase reporter assays showing the dose-dependent effect of CREB1 overexpression on CCAT1-CBS1, CCAT1-CBS2 and E2F1-CBS. (K) Semiquantitative ChIP-PCR assays demonstrating an *in vivo* interaction between CREB1 and the potential CREB1 binding site of CCAT1 and E2F1. The CREB1 binding site in the FOS gene promoter was used as a positive control, and the first intronic region of E2F1 was used as a negative control (Neg). (L) Quantitative gene expression analysis of CCAT1, CCAT1-L and MYC in HCT116 cells by dCas9-VP64 (CRISPRa) and dCas9-KRAB (CRISPRi) cotransfected with sgRNAs targeted upstream or downstream of the CCAT1 transcription start site, respectively. The data are representative of three independent experiments. Error bars represent SEM. *$p < 0.05$, as assessed by Student's *t*-tests.

Figure 4. Knockout of CREB1 induces the EMT phenotype by activating the NF-κB pathway via competition of coactivators CBP/p300. (A-B) qPCR (A) and Western blot (B) analyses of EMT marker RNA and protein levels in HCT116 and KO-CREB1 cells. (C) qPCR analysis of NF-κB pathway target genes upon knockout of CREB1 in HCT116 cells. (D) NF-κB reporter assays upon CREB1 overexpression in HCT116 and restoration in KO-CREB1 cells. (E-F) qPCR (E) and Western blot (F) analyses of the expression of EMT markers after treatment of both HCT116 and KO-CREB1 cells with a NF-κB pathway inhibitor. (G) Transwell migration

and invasion assays were performed to evaluate the migratory and invasive ability of both HCT116 and KO-CREB1 cells treated with NF-κB pathway inhibitors. Quantification of the cells was determined for plots and is represented on the right panel. (H) The regions of the p65-binding site of related EMT markers were quantified and were normalized to input levels following CBP and p300 ChIP-qPCR assays, which were performed on both HCT116 and KO-CREB1 cells. The data are representative of three independent experiments. Error bars represent SEM. *$p < 0.05$, as assessed by Student's *t*-tests.

Figure 5. A functional model of CREB1 for controlling transition of tumour cells between proliferation and metastatic states by transactivation of lncRNA CCAT1 and competition of coactivators CBP/p300.

Figure 1

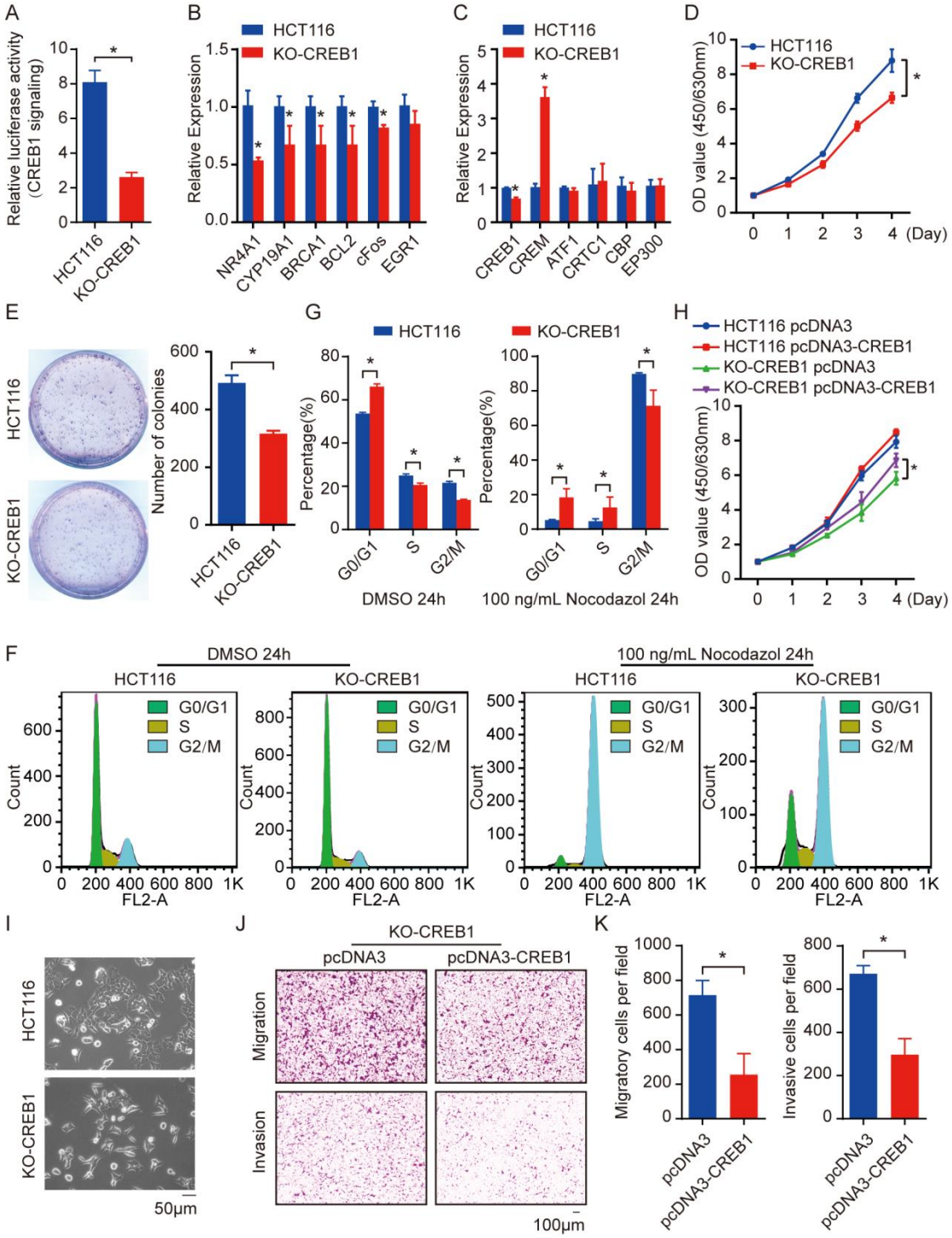
A
Relative luciferase activity (CREB1 signaling)
HCT116
KO-CREB1
B
HCT116
KO-CREB1
Relative Expression
NR4A1
CYP19A1
BRCA1
BCL2
cFos
EGR1
C
HCT116
KO-CREB1
Relative Expression
CREB1
CREM
ATF1
CRTC1
CBP
EP300
D
HCT116
KO-CREB1
OD value (450/630nm)
(Day)
E
HCT116
KO-CREB1
Number of colonies
G
HCT116
KO-CREB1
Percentage(%)
G0/G1
S
G2/M
DMSO 24h
100 ng/mL Nocodazol 24h
H
HCT116 pcDNA3
HCT116 pcDNA3-CREB1
KO-CREB1 pcDNA3
KO-CREB1 pcDNA3-CREB1
OD value (450/630nm)
(Day)
F
DMSO 24h
100 ng/mL Nocodazol 24h
HCT116
KO-CREB1
G0/G1
S
G2/M
Count
FL2-A
I
HCT116
KO-CREB1
50μm
J
KO-CREB1
pcDNA3
pcDNA3-CREB1
Migration
Invasion
100μm
K
Migratory cells per field
Invasive cells per field
pcDNA3
pcDNA3-CREB1

Figure 2

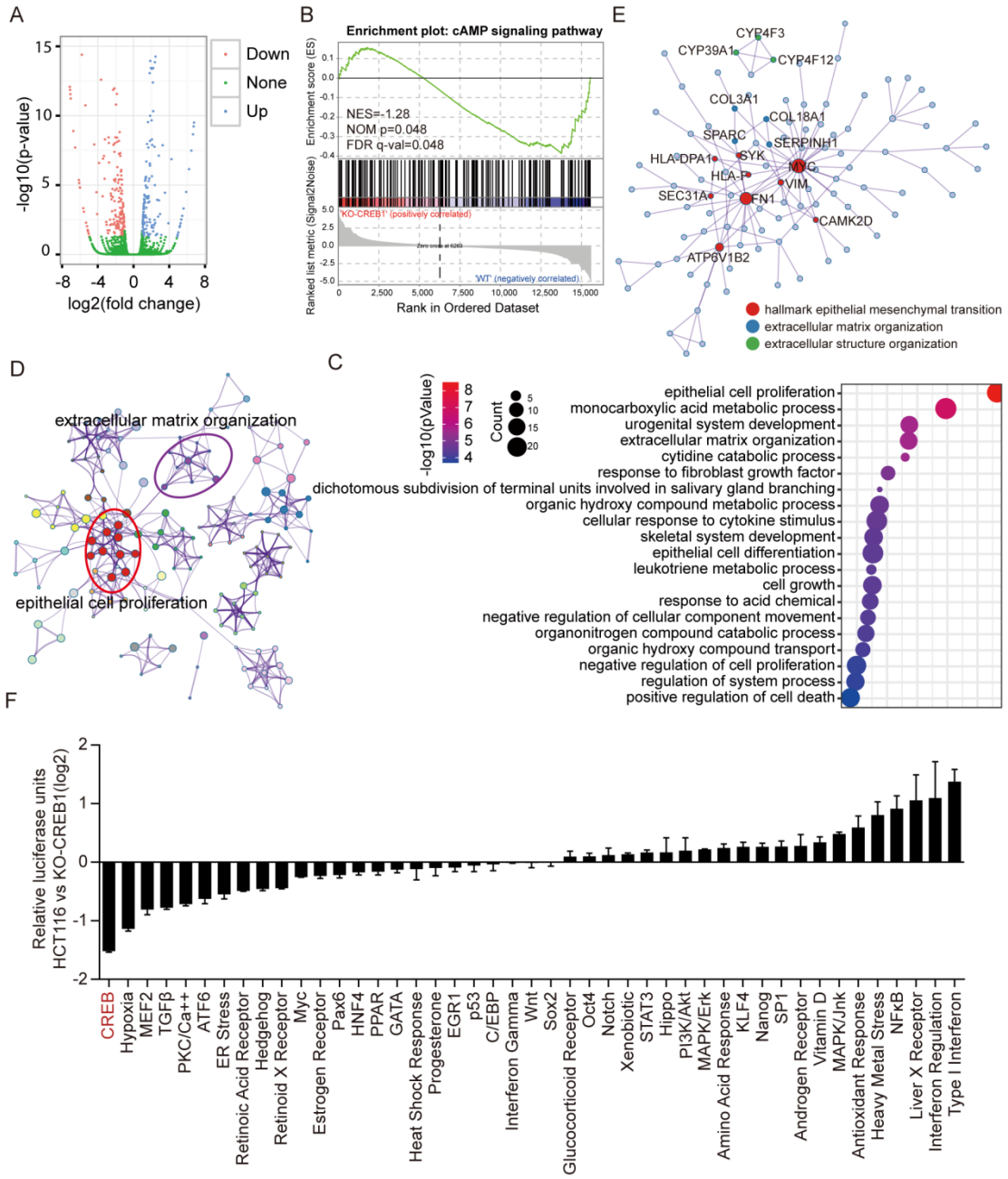
A
Down
None
Up
-log10(p-value)
log2(fold change)
B
Enrichment plot: cAMP signaling pathway
NES=-1.28
NOM p=0.048
FDR q-val=0.048
Enrichment score (ES)
Ranked list metric (Signal2Noise)
'KO-CREB1' (positively correlated)
'WT' (negatively correlated)
Rank in Ordered Dataset
E
CYP4F3
CYP39A1
CYP4F12
COL3A1
COL18A1
SPARC
SERPINH1
HLA-DPA1
SYK
HLA-F
VIM
SEC31A
FN1
CAMK2D
ATP6V1B2
hallmark epithelial mesenchymal transition
extracellular matrix organization
extracellular structure organization
D
extracellular matrix organization
epithelial cell proliferation
C
-log10(pValue)
Count
epithelial cell proliferation
monocarboxylic acid metabolic process
urogenital system development
extracellular matrix organization
cytidine catabolic process
response to fibroblast growth factor
dichotomous subdivision of terminal units involved in salivary gland branching
organic hydroxy compound metabolic process
cellular response to cytokine stimulus
skeletal system development
epithelial cell differentiation
leukotriene metabolic process
cell growth
response to acid chemical
negative regulation of cellular component movement
organonitrogen compound catabolic process
organic hydroxy compound transport
negative regulation of cell proliferation
regulation of system process
positive regulation of cell death
F
Relative luciferase units
HCT116 vs KO-CREB1(log2)
CREB
Hypoxia
MEF2
TGFβ
PKC/Ca++
ATF6
ER Stress
Retinoic Acid Receptor
Hedgehog
Retinoid X Receptor
Myc
Estrogen Receptor
Pax6
HNF4
PPAR
GATA
Heat Shock Response
Progesterone
EGR1
p53
C/EBP
Interferon Gamma
Wnt
Sox2
Glucocorticoid Receptor
Oct4
Notch
Xenobiotic
STAT3
Hippo
PI3K/Akt
MAPK/Erk
Amino Acid Response
KLF4
Nanog
SP1
Androgen Receptor
Vitamin D
MAPK/Jnk
Antioxidant Response
Heavy Metal Stress
NFκB
Liver X Receptor
Interferon Regulation
Type I Interferon

Figure 3

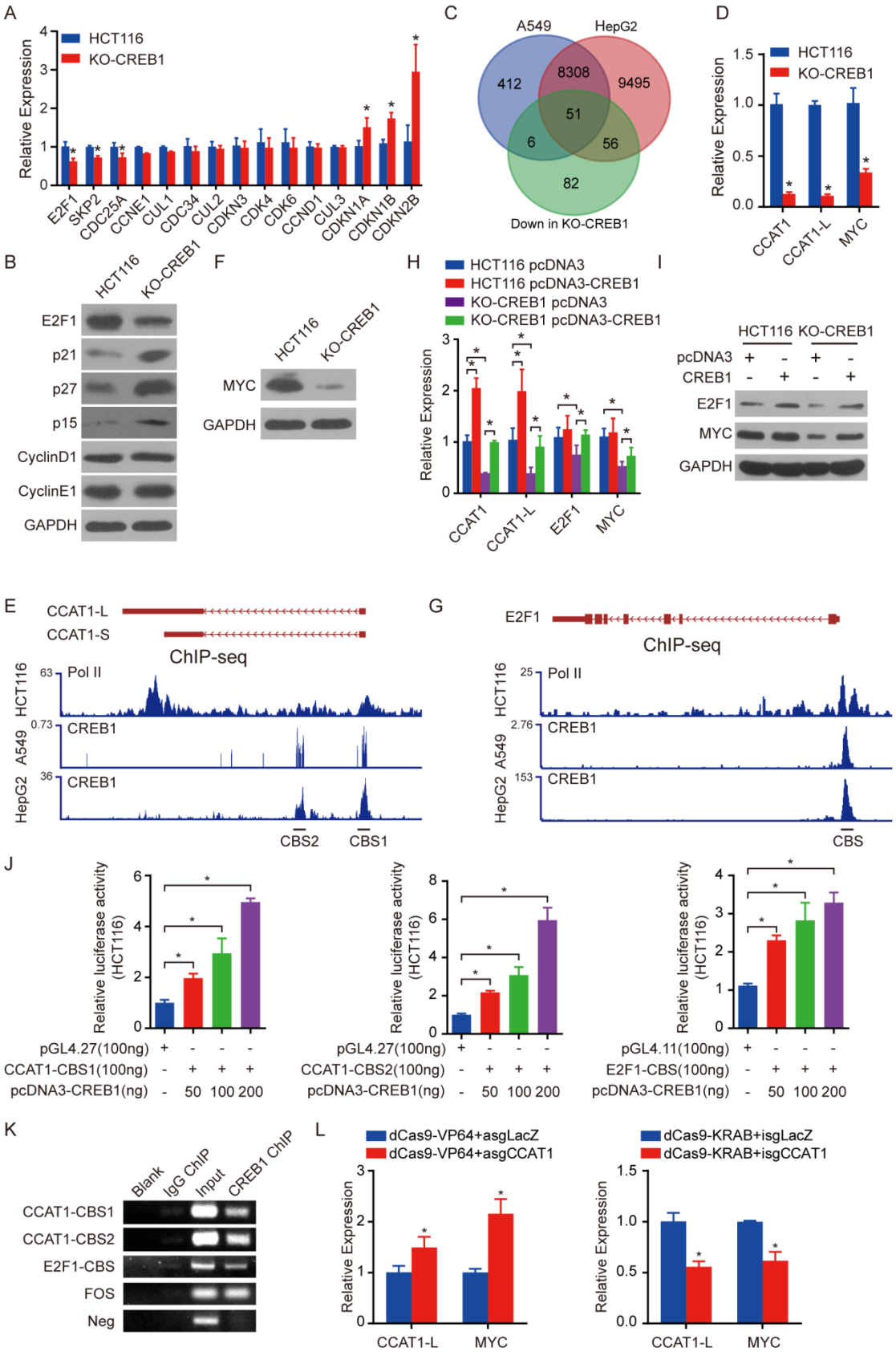
A
HCT116
KO-CREB1
Relative Expression
E2F1
SKP2
CDC25A
CCNE1
CUL1
CDC34
CUL2
CDKN3
CDK4
CDK6
CCND1
CUL3
CDKN1A
CDKN1B
CDKN2B
C
A549
HepG2
412
8308
9495
51
6
56
82
Down in KO-CREB1
D
HCT116
KO-CREB1
Relative Expression
CCAT1
CCAT1-L
MYC
B
HCT116
KO-CREB1
E2F1
p21
p27
p15
CyclinD1
CyclinE1
GAPDH
F
HCT116
KO-CREB1
MYC
GAPDH
H
HCT116 pcDNA3
HCT116 pcDNA3-CREB1
KO-CREB1 pcDNA3
KO-CREB1 pcDNA3-CREB1
Relative Expression
CCAT1
CCAT1-L
E2F1
MYC
I
HCT116 KO-CREB1
pcDNA3
CREB1
E2F1
MYC
GAPDH
E
CCAT1-L
CCAT1-S
ChIP-seq
Pol II
CREB1
HCT116
A549
HepG2
CBS2
CBS1
G
E2F1
ChIP-seq
Pol II
CREB1
HCT116
A549
HepG2
CBS
J
Relative luciferase activity (HCT116)
pGL4.27(100ng)
CCAT1-CBS1(100ng)
pcDNA3-CREB1(ng)
CCAT1-CBS2(100ng)
pGL4.11(100ng)
E2F1-CBS(100ng)
50 100 200
K
Blank
IgG ChIP
Input
CREB1 ChIP
CCAT1-CBS1
CCAT1-CBS2
E2F1-CBS
FOS
Neg
L
dCas9-VP64+asgLacZ
dCas9-VP64+asgCCAT1
dCas9-KRAB+isgLacZ
dCas9-KRAB+isgCCAT1
Relative Expression
CCAT1-L
MYC

Figure 4

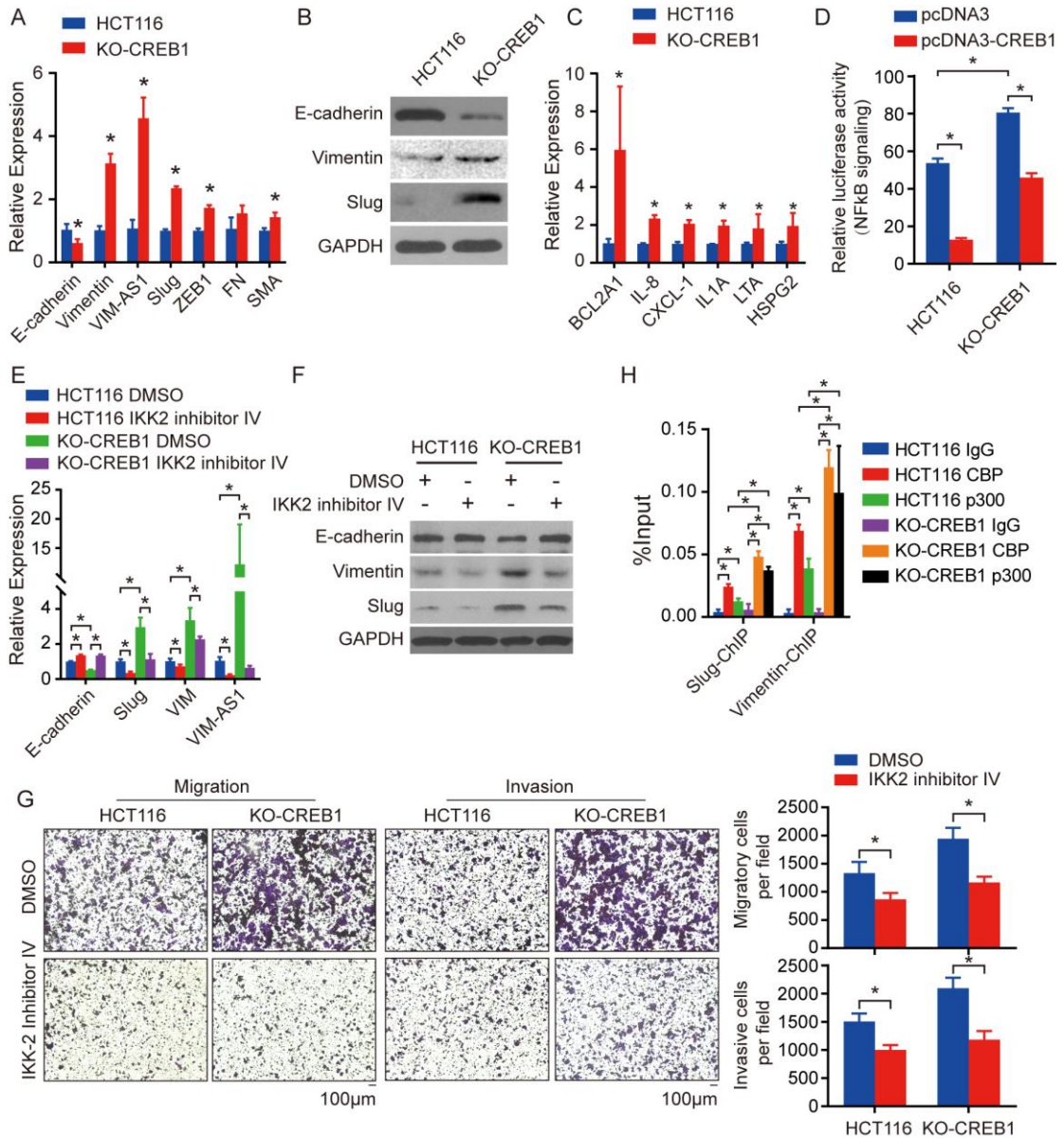
A
HCT116
KO-CREB1
Relative Expression
E-cadherin
Vimentin
VIM-AS1
Slug
ZEB1
FN
SMA
B
HCT116
KO-CREB1
E-cadherin
Vimentin
Slug
GAPDH
C
HCT116
KO-CREB1
Relative Expression
BCL2A1
IL-8
CXCL-1
IL1A
LTA
HSPG2
D
pcDNA3
pcDNA3-CREB1
Relative luciferase activity (NFkB signaling)
HCT116
KO-CREB1
E
HCT116 DMSO
HCT116 IKK2 inhibitor IV
KO-CREB1 DMSO
KO-CREB1 IKK2 inhibitor IV
Relative Expression
E-cadherin
Slug
VIM
VIM-AS1
F
HCT116
KO-CREB1
DMSO
IKK2 inhibitor IV
E-cadherin
Vimentin
Slug
GAPDH
H
%Input
HCT116 IgG
HCT116 CBP
HCT116 p300
KO-CREB1 IgG
KO-CREB1 CBP
KO-CREB1 p300
Slug-ChIP
Vimentin-ChIP
G
Migration
Invasion
HCT116
KO-CREB1
DMSO
IKK-2 Inhibitor IV
100μm
DMSO
IKK2 inhibitor IV
Migratory cells per field
Invasive cells per field
HCT116
KO-CREB1

Figure 5

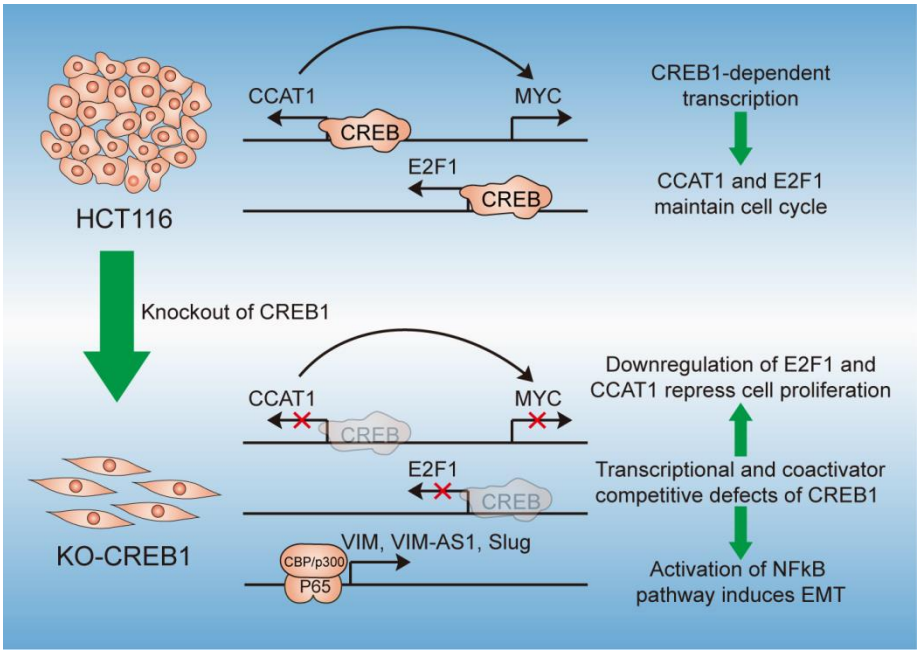
HCT116
CCAT1
MYC
CREB
E2F1
CREB
CREB1-dependent transcription
CCAT1 and E2F1 maintain cell cycle
Knockout of CREB1
KO-CREB1
CCAT1
MYC
CREB
E2F1
CREB
VIM, VIM-AS1, Slug
CBP/p300
P65
Downregulation of E2F1 and CCAT1 repress cell proliferation
Transcriptional and coactivator competitive defects of CREB1
Activation of NFkB pathway induces EMT